

# ***In Vivo* Label-free Confocal Imaging of Adult Mouse Brain Up to 1.3-mm Depth with NIR-II Illumination**

Fei Xia<sup>1,2,5</sup>, Chunyan Wu<sup>1,3,5</sup>, David Sinefeld<sup>1</sup>, Bo Li<sup>1</sup>, Yifan Qin<sup>1,4</sup>, Chris Xu<sup>1,\*</sup>

<sup>1</sup>School of Applied and Engineering Physics, Cornell University, Ithaca, NY, 14853, USA <sup>2</sup>Meinig School of Biomedical Engineering, Cornell University, Ithaca, NY, 14853, USA <sup>3</sup>College of Veterinary Medicine, Cornell University, Ithaca, NY, 14853, USA <sup>4</sup>National Key Laboratory of Science and Technology on Tunable Laser, Harbin Institute of Technology, Harbin 150080, China

<sup>5</sup>These authors contributed equally \*cx10@cornell.edu

## **ABSTRACT**

We combined NIR-II illumination at  $\sim 1.7 \mu\text{m}$  with reflectance confocal microscopy and achieved an imaging depth of  $\sim 1.3 \text{ mm}$  with high spatial resolution in adult mouse brain *in vivo*, which is 3-4 times deeper than that of conventional confocal microscopy using visible wavelength. We showed that the method can be added as an additional channel to any laser-scanning microscope with low-cost sources and detectors, such as continuous-wave (CW) diode lasers and InGaAs photodiodes. The technique is label-free, simple and requires low illumination power, potentially creating new opportunities for deep tissue imaging in various biological and clinical applications.

**Keywords:** Deep tissue imaging, confocal imaging, reflectance confocal microscopy, NIR-II region

## **1. INTRODUCTION**

Optical imaging through turbid medium such as biological tissues has long been a challenge due to strong scattering and absorption of light. One of the most fascinating problems is *in vivo* deep imaging of mouse brain with high resolution. A standard tool is multiphoton microscopy (MPM) because of its advantage in spatially-confined excitation volume and long excitation wavelength. Imaging mouse brains with 2-photon microscopy (2PM) [1] and 3-photon microscopy (3PM) [2] at beyond 1-mm depth *in vivo* were reported previously by leveraging the optimal wavelength windows for deep tissue penetration, i.e.  $1.3 \mu\text{m}$  and  $1.7 \mu\text{m}$ , determined by the combined effect of the scattering and absorption of brain tissues *in vivo*. Previous research has also shown that using optical coherence tomography (OCT) [3] and optical coherence microscopy (OCM) [4] with  $\sim 1.7 \mu\text{m}$  illumination could achieve an imaging depth up to 1.2 mm in mouse brain. However, for both OCT and OCM, time or coherence gating is needed for depth discrimination. We recently demonstrated *in vivo* reflectance confocal imaging of mouse brain at more than 1-mm depth with illumination wavelength at  $1.65 \mu\text{m}$  in the NIR-II region (1000-1700 nm) [5]. The power requirement for imaging deep mouse white matter is low (approximately tens of microwatts when using a PMT detector and tens of milliwatts when using an InGaAs photodiode detector). Furthermore, we compared the image contrast by performing simultaneous reflectance confocal and third-harmonic generation (THG) imaging. The images were well-correlated, particularly in the white matter region, indicating that reflectance confocal microscopy of the white matter may provide similar information as THG microscopy, but with a much simpler setup that only requires a low-cost CW diode laser as the illumination source. The long wavelength confocal microscopy demonstrated in this paper is simple and robust; and achieves high spatial resolution ( $\sim 1 \mu\text{m}$ ) at depth comparable to MPM and OCT, which is 3 to 4 times deeper than previously reported reflectance confocal imaging [6]. The method is label-free and can be easily added to any long wavelength 2PM and 3PM by the addition of a confocal detector.

## 2. METHODS

The imaging setup is the same as conventional reflectance confocal microscope, except that we set an additional detection channel for collecting THG signal for comparison (Fig.1). A polarization beamsplitter and a quarter-waveplate combination was installed to separate the illumination and back-scattered light. To explore the maximum imaging depth with the long wavelength, we first used a pulsed laser (Opera-F, Coherent) operating at 1650 nm as the illumination source and an InGaAs PMT (H10330C-75, Hamamatsu) as the detector. The back-scattered light is descanned and refocused into a multimode fiber (25 $\mu$ m-diameter core) by a 75-mm achromatic lens. The fiber core acted as the confocal pinhole. Low cost CW diode lasers and photodiode detectors can also be used for confocal imaging only.

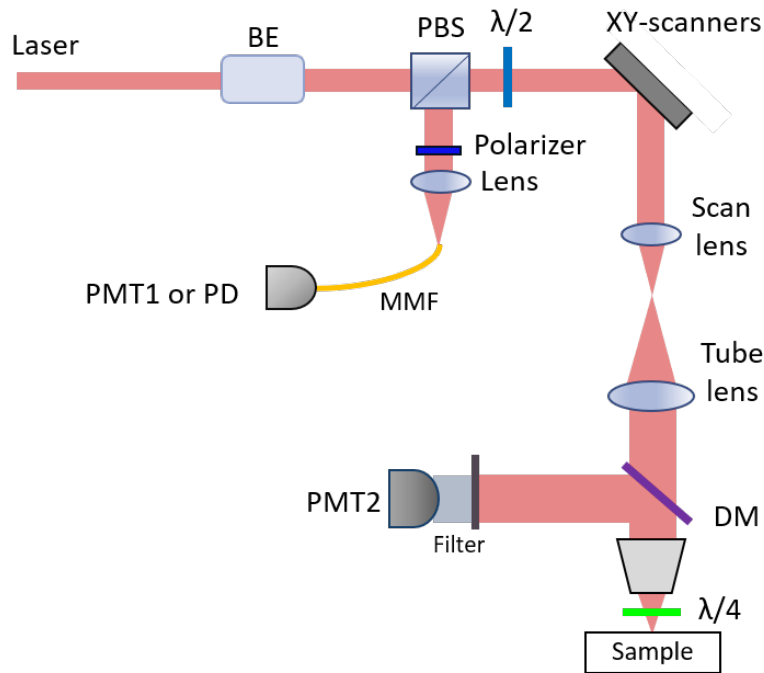


Figure 1. Schematic illustration of the imaging system. BE: beam expander, PBS: polarizing beam splitter,  $\lambda/2$ : half-waveplate,  $\lambda/4$ : quarter-waveplate, MMF: multimode fiber, DM: dichroic mirror. The focal length for the scan lens and tube lens is 150 mm and 750 mm, respectively. The photocathode for PMT1 and PMT2 is, respectively, InGaAs and ultra bialkali. An InGaAs photodiode (PD) is also used for some of the experiments.

We used CW laser diodes operating at 1610 nm (ILX Lightwave), 1630 nm and 1310 nm (FPL1059P, FPL1053P, respectively, Thorlabs), and a 70- $\mu$ m active area InGaAs photodiode (PD, Edmund Optics). A 150 mm-lens was used to refocus the back-scattered light onto the PD. We imaged wide-type C57BL/6J mice (16 to 32 weeks old) with 5-mm cranial windows centered at 2.2 mm lateral and 2 mm caudal from the bregma point. The optical power and integration time are tuned based on the detector gain and detector type. One of the challenging problems for RCM is the spurious reflection from the optical components in the beam path. While a PBS and  $\lambda/4$ -waveplate combination can largely suppress the spurious reflection from the optics before the  $\lambda/4$ -waveplate, we found that the back-reflection from the objective lens severely limits our ability to image deep. We used a 5  $\times$  5 mm square-shaped  $\lambda/4$ -waveplate (WPQ501, Thorlabs) instead of the normal cover-glass as the cranial window. The  $\lambda/4$ -plate cranial window has thickness close to a conventional cover glass ( $\sim$ 170  $\mu$ m), making it compatible with most microscope objectives. Since the  $\lambda/4$ -plate is placed after the objective lens, our PBS and  $\lambda/4$ -plate combination largely eliminates the back-reflection from the objective lens.

### 3. RESULTS

Figure 2 shows the comparison of the THG and reflectance confocal images obtained simultaneously *in vivo*. Within the mouse neocortex and external capsule (EC), the THG and reflectance confocal images have similar appearance, and both show the structure of the white matter and blood vessels.

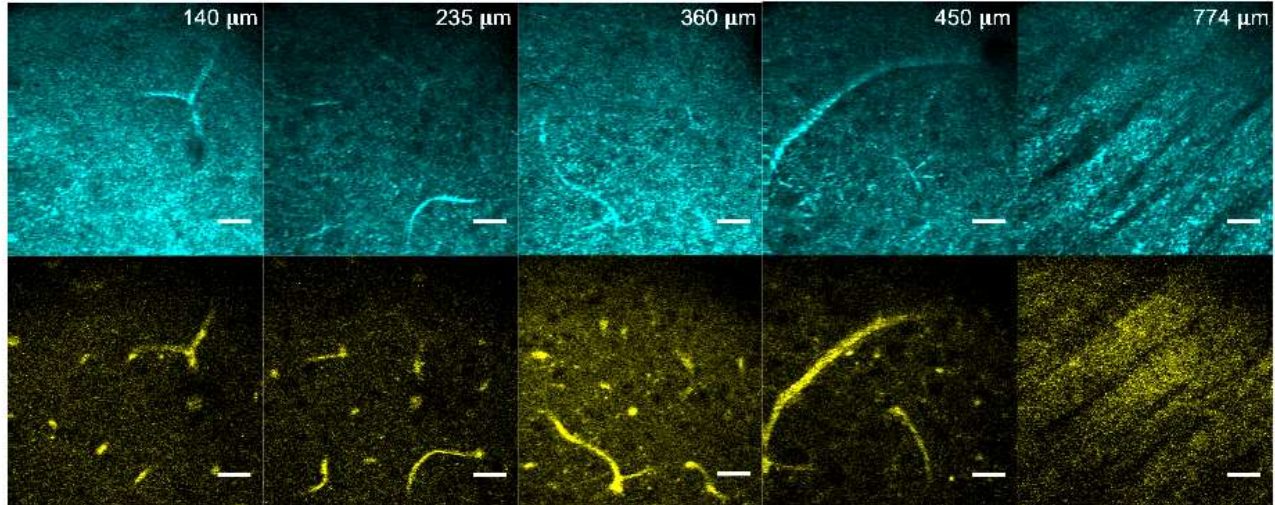


Figure 2. Comparison of THG (Top) and reflectance confocal (bottom) images of mouse cortex at various depths. Scale bars are 30  $\mu\text{m}$ .

As shown in Figure 3a, the maximum depth we could reach is  $\sim 1.3$  mm, through the entire neocortex and the EC (white matter region). The alveus of the hippocampus is observed from 1.2 mm to 1.3 mm below the brain surface. Semi-logarithmic plot of reflectance confocal signal (normalized to the signal at the surface and to the optical power) as a function of imaging depth in Figure 3b indicates the strongest signal comes from the white matter area of mouse brain which have densely packed myelinated axons. The imaging resolution is  $\sim 1$   $\mu\text{m}$  in lateral direction and  $\sim 3.4$   $\mu\text{m}$  in axial direction (Fig. 3c). We compared the illumination power for imaging the white matter using the PMT and the PD at approximately the same location of the same mouse. The brightness of the images obtained with  $\sim 30$   $\mu\text{W}$  (power at the surface of the mouse brain) using the PMT is comparable to images obtained with  $\sim 15$  mW using the PD (Fig. 3e). The maximum frame rate of our current set up is limited by the galvo-scanner to  $\sim 1.7$  Hz with  $512 \times 512$  pixels/frame (Fig. 3d) but can be improved significantly by using resonant scanners (e.g., 30 frames/s). In Fig. 3f, we show the confocal images of white matter under CW and pulsed laser illumination with the same power at 1310 nm, 1610 nm, 1630 nm and 1650 nm. Low cost CW diode lasers are clearly adequate as the illumination source for deep confocal imaging at the long wavelength windows.

### 4. CONCLUSIONS

In summary, we demonstrate *in vivo* deep brain reflectance confocal microscopy (RCM) with illumination at 1650 nm. The method is simple and robust, achieves spatial resolution ( $\sim 1$   $\mu\text{m}$ ) and imaging depth ( $> 1.2$  mm) comparable to MPM, and can be easily added to any long wavelength 2PM and 3PM by the addition of a confocal detector. Simultaneous THG and reflectance confocal imaging at NIR-II region were performed and the images obtained were similar but not identical, indicating additional information regarding the tissue properties at depth can be revealed. The advantages of the RCM at long wavelength illumination are confirmed by images acquired at various wavelengths, its simplicity of using photodiodes as detection sources and CW lasers as illumination sources, and its low power requirement compared to MPM. Comparing to other label-free methods such as THG, OCM [5], coherent anti-Stokes Raman scattering (CARS) microscopy [7], our method does not require expensive laser sources or complicated optical setup. The RCM at NIR-II illumination demonstrated in this paper can potentially be translated to other tissue types beyond the brain, for example, skin imaging [8, 9, 10], cancer diagnosis [11], and dynamic functional imaging, such as

blood flow imaging [12]. It has the promise to create new opportunities where high-resolution, label-free, deep imaging of tissue structure and function is required.

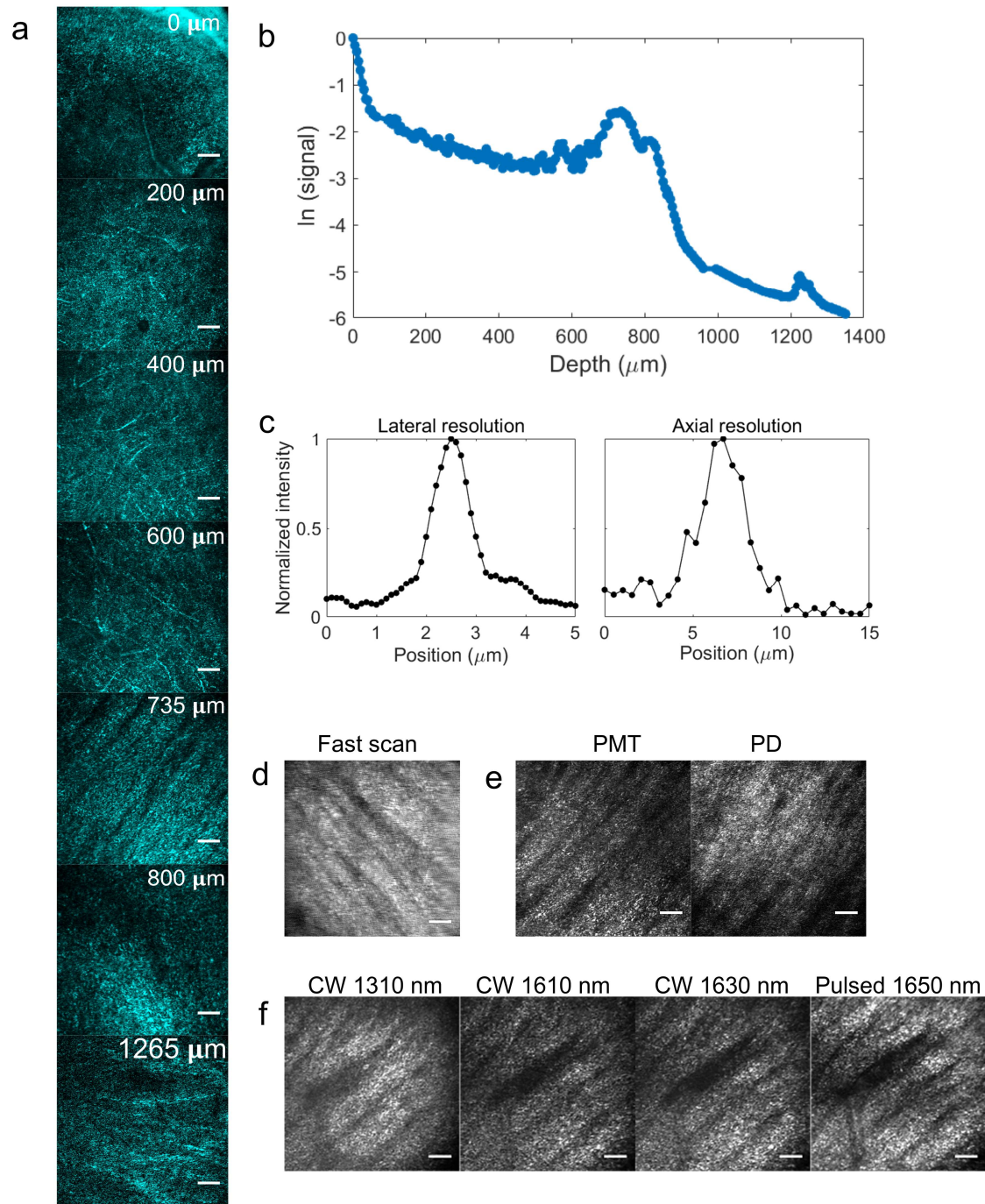


Figure 3. (a) *In vivo* reflectance confocal images at various depths. (b) Semi-logarithmic plot of reflectance confocal signal (normalized to the signal at the surface and to the optical power) as a function of imaging depth. (c) Lateral and axial intensity profiles of a small feature at ~340 μm depth. The lateral and axial FWHM is 1 μm and 3.4 μm, respectively. (d) White matter image at 810 μm depth acquired with ~1.7 Hz frame rate with 2 mW at the brain surface. (e) Confocal images of the white matter using the PMT (with ~30 μW at brain surface) and the PD (~15 mW) at approximately the same location of the same mouse. (f) Confocal images of white matter under CW and pulsed laser illumination with the same power at 1310 nm, 1610 nm, 1630 nm, and 1650 nm. The scale bars are 30 μm.

## REFERENCES

- [1] Kobat, D., Horton, N.G. and Xu, C., “In vivo two-photon microscopy to 1.6-mm depth in mouse cortex,” *J of Biomed. Opt.*, 16(10), p.106014. (2011)
- [2] Horton, N.G., Wang, K., Kobat, D., Clark, C.G., Wise, F.W., Schaffer, C.B. and Xu, C., “In vivo three-photon microscopy of subcortical structures within an intact mouse brain,” *Nat. photon.*, 7(3), p.205. (2013)
- [3] Chong, S.P., Merkle, C.W., Cooke, D.F., Zhang, T., Radhakrishnan, H., Krubitzer, L. and Srinivasan, V.J.,” Noninvasive, in vivo imaging of subcortical mouse brain regions with 1.7  $\mu\text{m}$  optical coherence tomography,” *Opt. letters*, 40(21), pp.4911-4914. (2015)
- [4] Yamanaka, M., Teranishi, T., Kawagoe, H. and Nishizawa, N., “Optical coherence microscopy in 1700 nm spectral band for high-resolution label-free deep-tissue imaging,” *Sci. rep.*, 6, p.31715. (2016)
- [5] Xia, F., Wu, C., Sinefeld, D., Li, B., Qin, Y. and Xu, C. “In vivo label-free confocal imaging of the deep mouse brain with long-wavelength illumination,” *Biomed. Opt. Exp.*, 9(12), pp.6545-6555. (2018)
- [6] Schain, A.J., Hill, R.A. and Grutzendler, J., “Label-free in vivo imaging of myelinated axons in health and disease with spectral confocal reflectance microscopy,” *Nat. med.*, 20(4), p.443. (2014)
- [7] Qin, Y., Li, B., Xia, F., Xia, Y. and Xu, C., “Multi-color background-free coherent anti-Stokes Raman scattering microscopy using a time-lens source,” *Opt. Express*, 26(26), pp.34474-34483. (2018)
- [8] Huzaira, M., Rius, F., Rajadhyaksha, M., Anderson, R. R., and González, S., “Topographic variations in normal skin, as viewed by in vivo reflectance confocal microscopy,” *J. Invest. Dermatol.* 116(6), 846–852 (2001).
- [9] Calzavara-Pinton. P., Longo, C., Venturini, M., Sala, R., and Pellacani, G., “Reflectance confocal microscopy for in vivo skin imaging,” *Photochem. Photobiol.* 84(6), 1421–1430 (2008).
- [10] Larson. B., Abeytunge, S., and Rajadhyaksha, M., “Performance of full-pupil line-scanning reflectance confocal microscopy in human skin and oral mucosa in vivo,” *Biomed. Opt. Express* 2(7), 2055–2067 (2011).
- [11] Woodward, R. M., Cole, B. E., Wallace, V. P., Pye, R. J., Arnone, D., Linfield, E. H., and Pepper, M., “Terahertz pulse imaging in reflection geometry of human skin cancer and skin tissue,” *Phys. Med. Biol.* 47(21), 3853–3863 (2002).
- [12] Kobat, D., Durst, M. E., Nishimura, N., Wong, A. W., Schaffer, C. B., and Xu, C., “Deep tissue multiphoton microscopy using longer wavelength excitation,” *Opt. Express* 17(16), 13354–13364 (2009).